10.5005/jp-journals-10003-1096
INVITED REVIEW ARTICLE

Imaging of Parapharyngeal Space and Infratemporal Fossa

Sanjay Jain, Aman Kumar, Harshal Dhongade, Ravi Varma

ABSTRACT

Cross-sectional imaging is an indispensable tool in the investigation of parapharyngeal space and infratemporal fossa pathologies. Computed tomography and magnetic resonance imaging exquisitely display the complex anatomy of this region and provides accurate spatial localization of pathology, differential diagnosis and vital information for treatment planning.

Keywords: Parapharyngeal space, Infratemporal fossa, Imaging.

How to cite this article: Jain S, Kumar A, Dhongade H, Varma R. Imaging of Parapharyngeal Space and Infratemporal Fossa. Int J Otorhinolaryngol Clin 2012;4(3):113-121.

Source of support: Nil

Conflict of interest: None declared

INTRODUCTION

The parapharyngeal space (PPS) is centrally located and surrounded by other neck spaces from all sides. Due to its critical location and anatomic relationships, it acts as a highway for spread of infection and tumors from any of the areas that surround it to any of the other bordering spaces. Clinical examination is limited by the inaccessible location; hence diagnosis of PPS pathologies is completely dependent on cross-sectional imaging.

PPS ANATOMY

PPS is an inverted pyramidal-shaped potential space extending down from the skull base on either side of the pharynx (Figs 1 and 2). It is divided into two compartments: Prestyloid and retrostyloid by tensor-vascular-styloid fascia.[1] This fascia connects tensor veli palatini muscle with

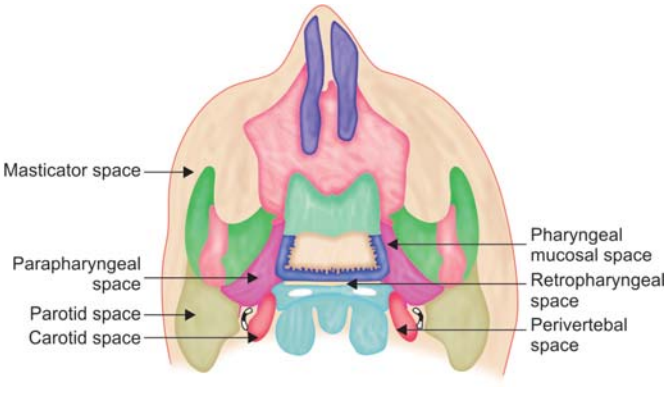

Fig. 1: Diagrammatic representation of suprahyoid neck spaces

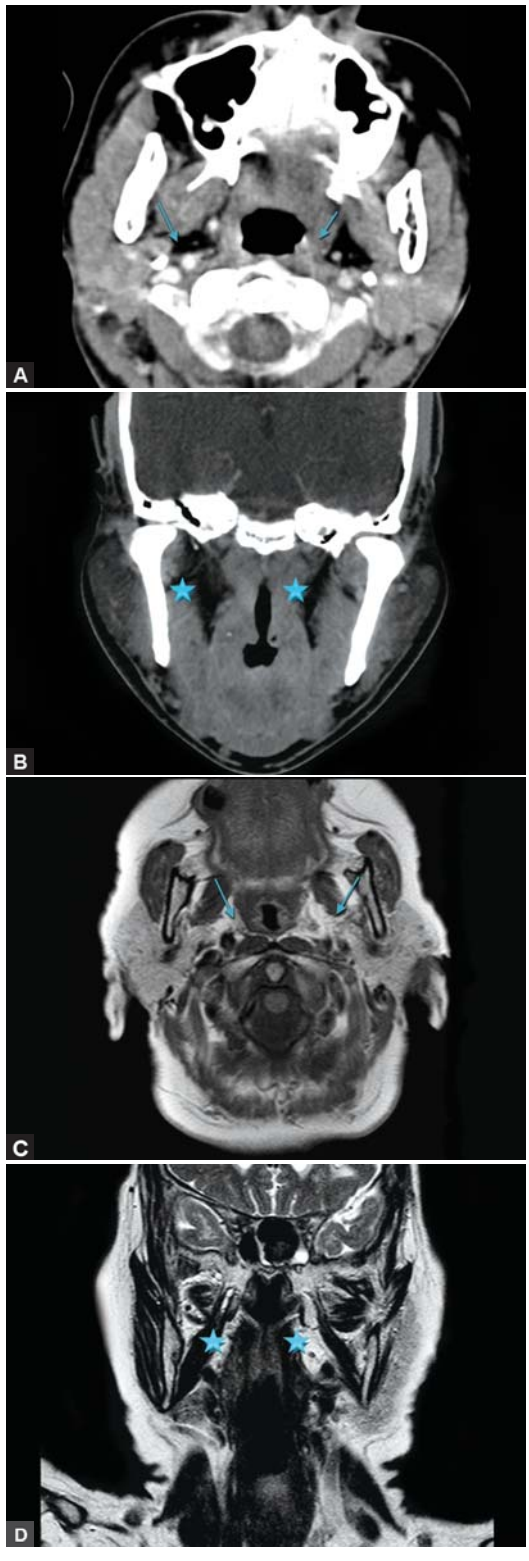

Figs 2A to D: Radiological anatomy of parapharyngeal space: An inverted pyramid-shaped space along the pharynx on either side (A and C: arrows) (B and D: ★) extending from skull base up to the level of angle of mandible

styloid process. Prestyloid compartment lies anterolateral to this fascia while retrostyloid compartment lies posteromedial to this fascia. The prestyloid compartment is filled with fat, connective tissue, minor or ectopic salivary glands, branches of the mandibular division of the trigeminal nerve, internal maxillary artery, ascending pharyngeal artery and pharyngeal venous plexus. The components of the retrostyloid compartment include the internal carotid artery, internal jugular vein, cranial nerves IX-XII, and cervical sympathetic chain and glomus bodies. This terminology for the PPS is most often used by surgeons.[1] Some radiologists separate the carotid space from the PPS and describe them as two separate spaces.[2,3]

The PPS is bounded medially by the buccopharyngeal fascia which covers the pharyngobasilar fascia and outer aspect of pharyngeal constrictor muscles. The anterior border is formed by the pterygomandibular raphe. The lateral boundary is formed by the fascia on the medial aspect of the masticator space and the fascia over the deep surface of the parotid gland. On the posteromedial aspect there is retropharyngeal space. The space extends inferiorly up to the styloglossus muscle at the level of angle of mandible. As there is no fascia separating the inferior PPS from the submandibular space, open communication exists between PPS and posterior submandibular space. Superiorly, the space interacts with the skull base in bland triangular area on the inferior surface of petrous apex.

The parotid space lies lateral to PPS while masticator space lies anterolaterally. Pharyngeal mucosal space lies medially while retropharyngeal space lies on the posteromedial aspect of the PPS. The stylomandibular tunnel is bounded by the posterior ramus of the mandible, the skull base and the stylomandibular ligament through which deep lobe of parotid protrudes into the PPS.

Infratemporal Fossa

The infratemporal fossa (ITF) is a larger space bounded anteriorly by the posterior surface of the maxilla, posteriorly by the mastoid temporal bone, laterally by the vertical ramus of mandible and zygomatic arch, superiorly by inferior surface of greater wing of sphenoid and squamous temporal bone, and medially by the sphenoid pterygoid process, pterygomaxillary fissure and lateral part of nasopharynx.[4] Inferiorly it is bounded by the superior limit of posterior belly of digastric and angle of the mandible and has no floor. The contents of the ITF are pterygoid muscles, internal maxillary artery, pterygoid venous plexus and mandibular division of trigeminal nerve. The masseter is not a content of the ITF. The nonfascial lined ITF thus combines a large part of the masticator space, PPS and the retroantral buccal space reaching up to the skull base superiorly.

PATHOLOGIES

Congenital/Developmental Lesions

Branchial cysts may arise in the PPS. They originate in the second branchial apparatus most likely from the branchial pouch.[5] These cysts are located deep to the tonsillar fossa in the medial aspect of the PPS and just anterior to retropharyngeal space. On computed tomography (CT) they are seen as low attenuation (10-20 HU) lesions with thin uniformly smooth wall. On magnetic resonance imaging (MRI), they appear as T1W hypointense and T2W hyperintense lesions with peripheral enhancement on postcontrast study. When a cyst is infected, the density of its content increases and shows increased attenuation on CT and the wall thickens and enhances.[6]

Teratomas may rarely occur in the PPS and most have occurred in newborns and infants and neonates. Components of all three germ layers are present. On CT, areas of calcification, ossification, fat and cystic degeneration can be seen within a heterogeneously enhancing mass lesion.[7]

Infections

PPS and infratemporal fossa infections mostly result from contiguous spread from other spaces. Common primary source of infections in such cases are masticator space (dental infections), maxillary sinus, peritonsillar space and submandibular space.[8]

Role of imaging in these cases is to confirm the presence of inflammation, delineate the extent of involvement and differentiate between cellulitis and abscess formation, which requires drainage. On imaging there will be enlargement of these spaces, fat stranding and obliteration of fat planes. On CT it appears as increased attenuation of fat and dirty appearing fat. On MRI T1W images show decreased signal of fat, while increased signal intensity is seen on T2W imaging, due to increased fluid content. Inflamed muscles appear hypodense on CT, show increased signal on T2W MRI and inhomogeneous postcontrast enhancement on both CT and MRI (Figs 3A to C).

An abscess is best identified with contrast enhanced imaging. On CT, it appears as a peripherally enhancing lesion with central nonenhancing hypodense core. On MRI, the necrotic core appears hypointense to intermediate signal on T1W imaging and hyperintense on T2W imaging with peripherally enhancing rim on postcontrast imaging. Identification of peripherally enhancing rim is important in differentiating abscess from phlegmon or cellulitis.

Neoplastic Lesions

Tumors of the PPS account for less than 0.5% of head and neck neoplasms.[9] They fall into three categories: Primary,

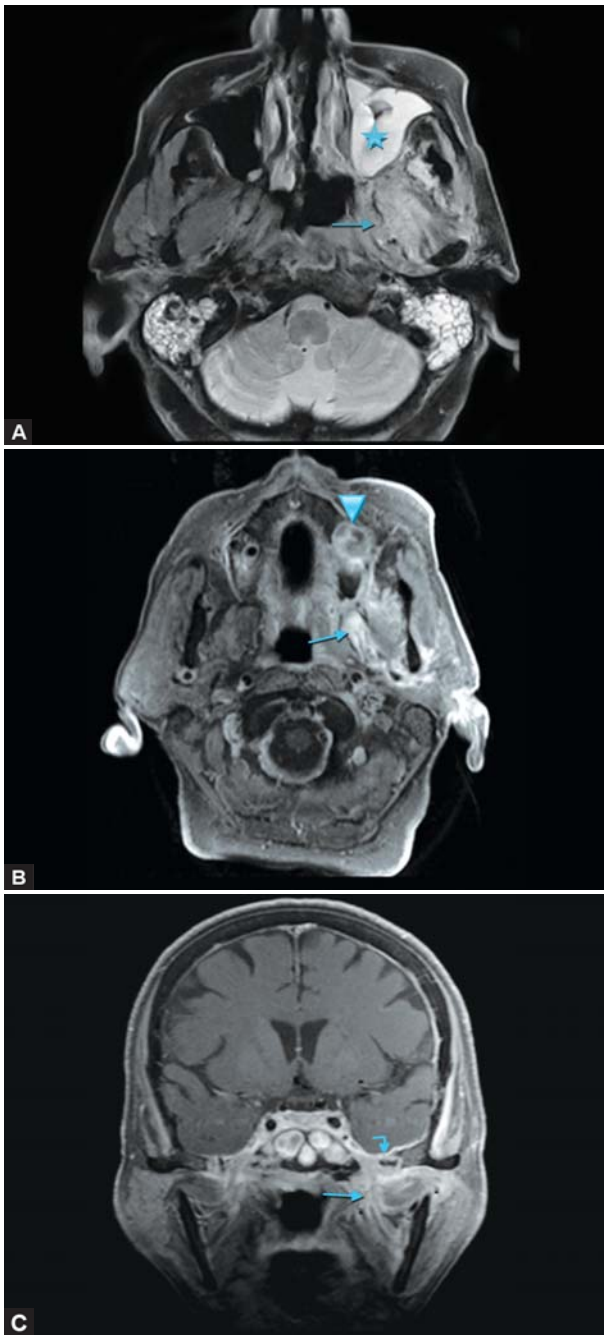

Figs 3A to C: Parapharyngeal space and infratemporal fossa infection: Diffuse ill-defined hyperintensity on T2W images (A: arrow) and heterogenous diffuse postcontrast enhancement (B: arrows) in the left infratemporal fossa and parapharyngeal space is suggestive of cellulitis. Infection has involved the skull base causing dural enhancement (C: curved arrow). Infection originated in the left upper alveolus (B: arrowhead) and has also involved the maxillary sinus (★)

metastatic and extension from adjacent structures. The vast majority of the lesions of the PPS arise in adjacent spaces and spread from there into the PPS.[6] To conclude that a lesion is primary to PPS, it must be surrounded by fat from all sides. The most common primary neoplasms to arise in the PPS are of salivary gland origin, next common being neurogenic tumors.[8]

Salivary Gland Tumors

Primary salivary gland tumors of PPS originate from minor salivary glands in the PPS. Pleomorphic adenoma is the most common tumor type.[8]

Pleomorphic adenoma (benign mixed tumor) appears as a well-defined rounded mass with smooth noninfiltrating margins. When larger than 2 cm they may have cystic or necrotic areas within them. On CT, small lesions appear as hypodense enhancing lesions. On MRI, they have isointense to intermediate T1-weighted and high T2-weighted signal intensities and show homogenous enhancement on

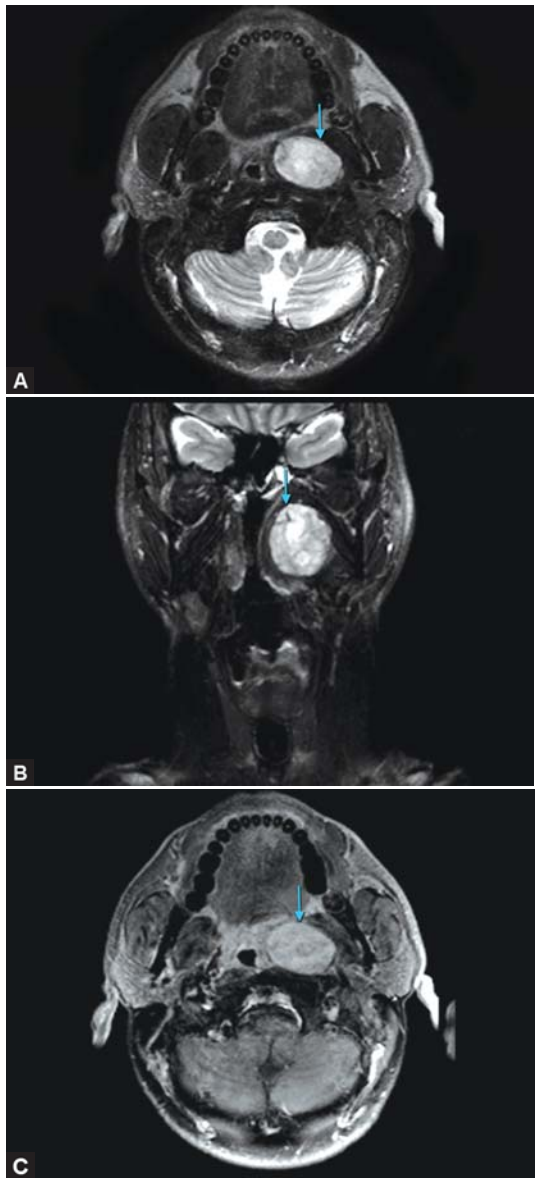

Figs 4A to C: Minor salivary gland tumor: An oval mass in prestyloid compartment of left parapharyngeal space. It appears heterogeneously hyperintense on T2W imaging (A and B: arrows) and shows heterogenous contrast enhancement (C). Imaging morphology was suggestive of a primary tumor of the parapharyngeal space, most likely to be a minor salivary neoplasm. Histopathology revealed a pleomorphic adenoma of minor salivary gland

postcontrast study (Figs 4A to C). It is important to look for intervening fat separating the tumor from the parotid gland to diagnose it as originating primarily from the PPS.

If the margins of tumor are not clearly defined, then possibility of uncommon malignancy like mucoepidermoid or adenoid cystic carcinoma is to be considered.

Salivary gland tumors are always anterior to the internal carotid artery (ICA) and, if large enough, will displace the ICA posteriorly.[10]

Neurogenic Tumors

Neurogenic tumors are the second most common neoplasms originating from the prestyloid PPS and are the most common retrostyloid PPS tumors.[8] These consist of schwannomas, neurofibromas and paragangliomas.

Schwannomas are much more common than neurofibromas. In prestyloid compartment, schwannoma originating from trigeminal nerve is common. In retrostyloid compartment, schwannoma originating from vagus nerve is common followed by glossopharyngeal nerve while that from sympathetic chain is rare.[6] Neurofibroma as such is rare and they are usually associated with neurofibromatosis.

Schwannoma

Schwannomas are fusiform, sharply circumscribed masses seen on CT as soft tissue density masses with few cystic areas within. They show uniform enhancement on postcontrast study. On MRI, they appear heterogeneously hyperintense on T2W images and isointense to hypointense on T1W images.[11] No flow voids are noted within them which help it differentiate from paraganglioma.

As schwannomas are hypovascular and have poor venous drainage, there is slow accumulation of contrast within the tumor and thus they show persistent and increased enhancement on delayed scans taken after 2 minutes of administration of contrast. This is in contrast to paraganglioma which is a hypervascular tumor and show early peak enhancement with rapid washout of contrast on delayed phases.[12,13] The third differentiating point between schwannoma and paraganglioma is that when the lesions extend through a skull base foramen, schwannoma will cause scalloping and smooth enlargement of the foramen while paragangliomas will cause irregular erosions of bony margins of foramen.

The nature of displacement of carotid vessels and internal jugular veins help in predicting the nerve of origin of schwannoma and also differentiating it from other benign lesions of PPS like minor salivary gland tumor.[14] In vagal nerve schwannoma, there is anteromedial displacement of ICA and posterolateral displacement of internal jugular vein (IJV) while in schwannoma arising from sympathetic chain, there is anterior displacement of both ICA and IJV.

Paraganglioma

They represent 10 to 15% of all the lesions in the PPS, almost all of them originating in the retrostyloid compartment. Three varieties of paraganglioma are seen in the PPS depending on its site of origin.[6] The most common type is glomus vagale paraganglioma originating from the glomus bodies located in nodose ganglion of vagus nerve just 1 to 2 cm below jugular foramen. Second common type is the carotid body tumor which originates from the carotid body cells near the carotid bifurcation. They cause characteristic splaying of ICA and ECA when located in the crux of carotid

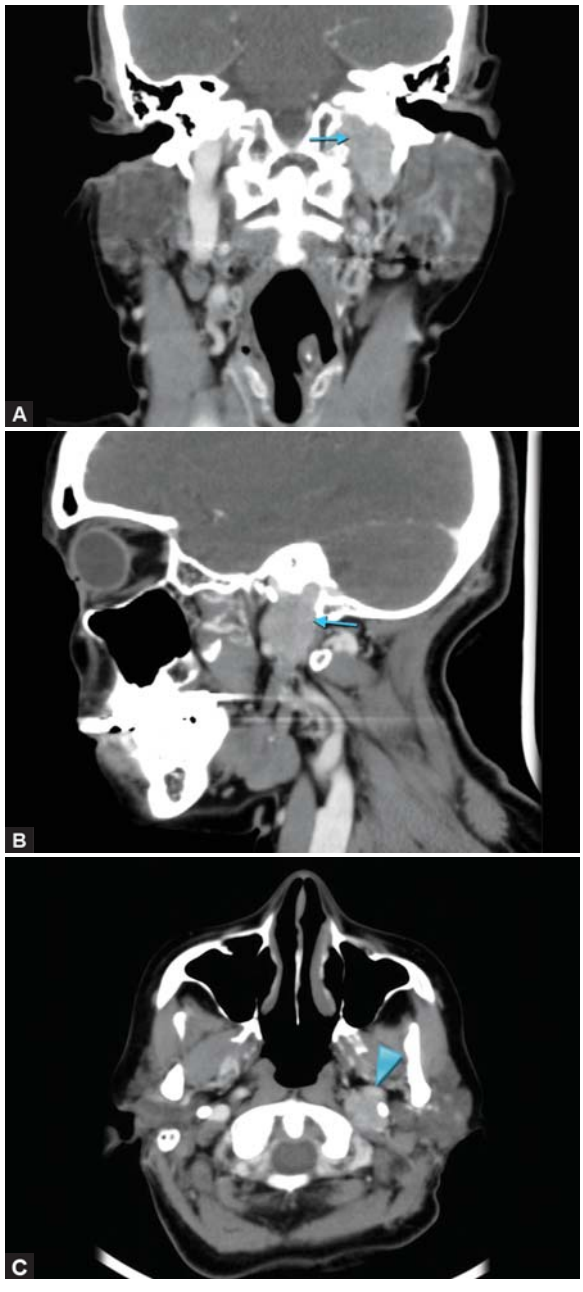

Figs 5A to C: Glomus jugulare paraganglioma: Contrast enhanced CT images show an enhancing elongated mass lesion (A and B: arrows) at the skull base extending from the jugular foramen to retrostyloid parapharyngeal space displacing the internal carotid artery anteriorly (C: arrowhead)

bifurcation, called the Lyre's sign.[15] Third type of paraganglioma of this region is glomus jugulare tumors (Figs 5A to C) which arise from the paraganglionic cells around the jugular ganglion. The bulk of the lesion, both above and below the skull base, is almost equal.

On imaging, paraganglioma appears as a smoothly contoured, ovoid PPS mass with multiple vascular flow voids noted in the lesion on spin echo sequences of MRI. In small lesions less than 2 cm, flow voids may not be seen. On T2W sequence, a characteristic 'salt and pepper' appearance is noted. The explanation for this appearance is that scattered high signal intensity foci are noted on T2W images due to the slow flow within the tumor and due to foci of subarachnoid hemorrhage within the lesion combined with serpentine low signal intensity areas corresponding to flow voids due to rapid flow in some of the vessels within the lesion.[16]

Dynamic contrast enhanced MRI further helps in characterizing a lesion as paraganglioma as it will show a hypervascular curve with a sharp early filling peak and a rapid washout phase.[12,13] A drop out phenomenon has been described by Vogt et al[17] for skull base paragangliomas. On dynamic MR scanning when images are taken at the same level, due to the hypervascularity of paragangliomas, there is high concentration of gadolinium reached in the tumor 24 to 42 seconds after start of injection such that due to susceptibility effect of gadolinium there is signal loss from the lesion. As the concentration of gadolinium slowly decreases, the signal intensity increases once again. Others tumors do not show this phenomenon.

On CT, as mentioned above, paragangliomas which extend into/through the skull base foramen will cause irregular erosions of the margin of the foramen.

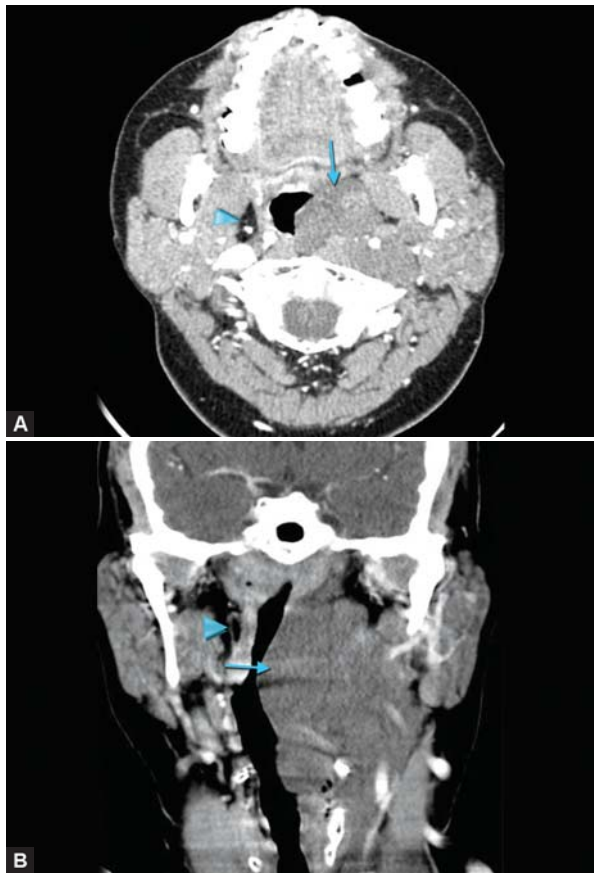

Figs 6A and B: Lymphangioma: Axial and coronal CT scan of a lymphangioma in the left side of neck insinuating into parapharyngeal space (A and B: arrows). The normal fat-filled parapharyngeal space is seen on the contralateral side (A and B: arrowheads)

Vascular Malformations

Vascular malformations result from aberrant development of vascular channels. These lesions are usually transpatial.

Lymphangiomas

Lymphangiomas (Figs 6A and B) presumably form due to sequestrations of embryonic lymph sacs. They are smooth nonencapsulated masses, consist of dilated endothelial lined lymphatic spaces and may have thin-walled vessels within them. On imaging they appear as unilocular or multilocular cystic masses with thin walls. They are usually trans-spatial and tend to insinuate between normal structures without causing mass effect. On CT they appear as hypodense poorly defined cystic masses. On MRI they are usually hypointense on T1W imaging; however they can be hyperintense if containing high proteinacious contents or blood. On T2W they appear hyperintense, transpatial lesions and it is the best sequence to delineate extent of lesion. Usually no significant postcontrast enhancement is seen on either CT or MRI, except mixed vascular and lymphatic lesions.

Venous Vascular Malformations

Venous vascular malformations or cavernous hemangiomas (Figs 7A to C) are the most common vascular malformations of head and neck. They arise due congenital arrest of vascular development.

Pathologically it is a conglomerated mass of venous channels of variable diameter. Intraluminal thrombi and phleboliths are commonly seen. On imaging it appears as lobulated soft tissue mass of variable size with phleboliths. It tends to infiltrate adjacent compartments, resulting in trans-spatial mass. On CT it appears as isodense lobulated soft tissue mass with round calcifications. Remodeling of adjacent bones can be seen. Postcontrast enhancement is variable, depending on intralesional flow rate. Enlarged draining vein can be seen on CT angiography, however feeding artery is difficult to identify. On MRI it appears from iso- to hypointense, multilobulated lesion. On T2W

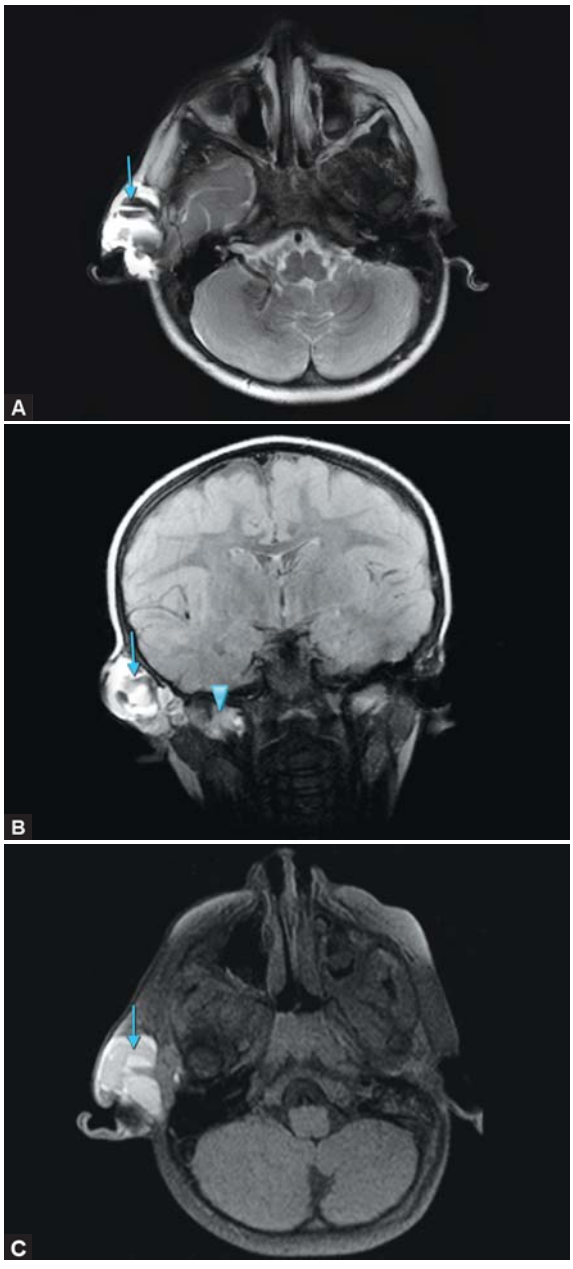

Figs 7A to C: Venous vascular malformation: A lobulated preauricular mass is seen extending into the parapharyngeal space (B: arrowhead). It is heterogeneously hyperintense on T2W image and shows serpiginous flow voids (A and B: arrows). On postcontrast imaging, the lesion enhances markedly and the serpiginous channels fill with contrast (C: arrow)

imaging it can appear as a septated hyperintense lesion, if consist of large vascular channels or solid lesion of intermediate signal intensity, if consist of small vascular channels. Rounded areas of signal loss due to phleboliths are usually seen. Postcontrast enhancement is variable, can be mild or intense, homogenous or heterogeneous. MR venography can show enlarged draining vein.[18]

Tumors Extending from Adjacent Spaces

In adults common infiltrative lesions to involve the infratemporal fossa are squamous cell carcinomas of the

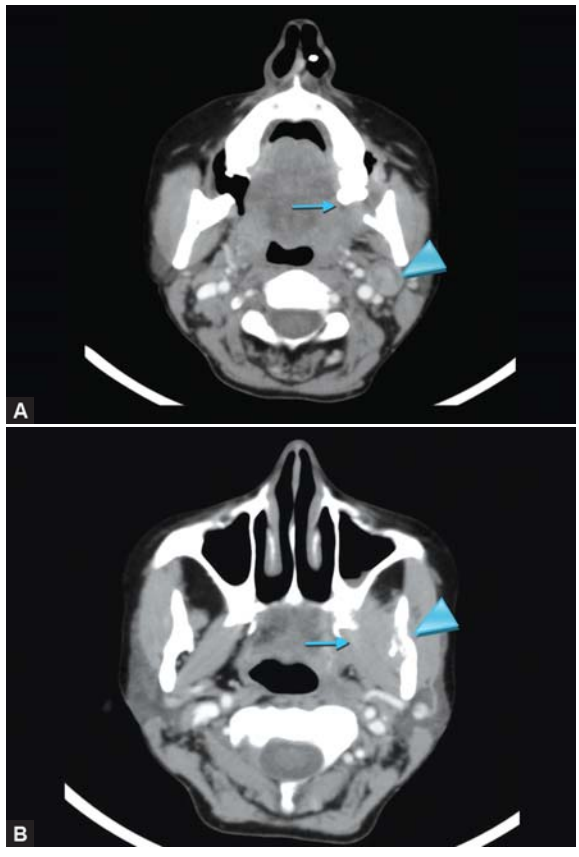

Figs 8A and B: Retromolar trigone squamous cell carcinoma: An ill-defined heterogeneously enhancing mass in left infratemporal fossa (A and B: arrows) with involvement of mandible (B: arrowhead). An enlarged left level II lymph node is also seen (A: arrowhead)

retromolar trigone (Figs 8A and B) and pharynx (Figs 9A to C) while in children it is rhabdomyosarcoma or lymphoma[19] (Figs 10A and B).

The prestyloid PPS is most commonly involved by salivary gland tumors arising from the deep lobe of the parotid gland.[8] A pleomorphic adenoma originating in the deep lobe of parotid and extending into the PPS will be seen as a dumbbell-shaped mass with waist at stylomandibular tunnel.

Mucoepidermoid and adenoid cystic carcinomas originating in the minor salivary glands of lateral pharyngeal wall and infiltrating into the prestyloid fat will have fat only on its lateral contour.

Other infiltrative lesions to spread to the PPS are sarcomas of fatty, muscular and fibrous origin arising from the adjacent spaces. Osseous and cartilaginous lesions arising from the skull base, cervical vertebrae and mandible like osteoma, osteochondroma, osteogenic sarcomas, chondromas, chondrosarcomas and chordomas may extend into PPS via stalk-like extension.

Rarely, primary intracranial neoplasms like meningiomas may extend into PPS via any of the skull base foramina (commonly jugular foramen) or by invading the skull base itself.[20] They appear as homogeneously enhancing

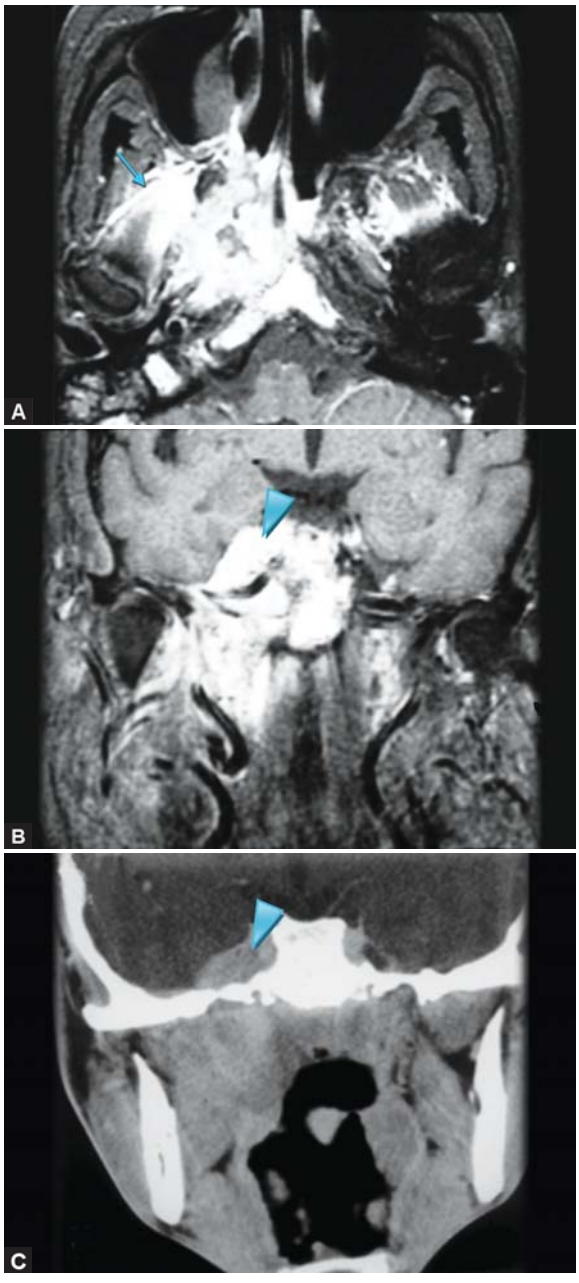

Figs 9A to C: Nasopharyngeal carcinoma: Contrast enhanced MRI (A—axial, B—coronal) and coronal CT (C) show an infiltrating enhancing mass in the right nasopharyngeal wall extending into right infratemporal fossa (A: arrow) and intracranially (B and C: arrowheads) into right parasellar region

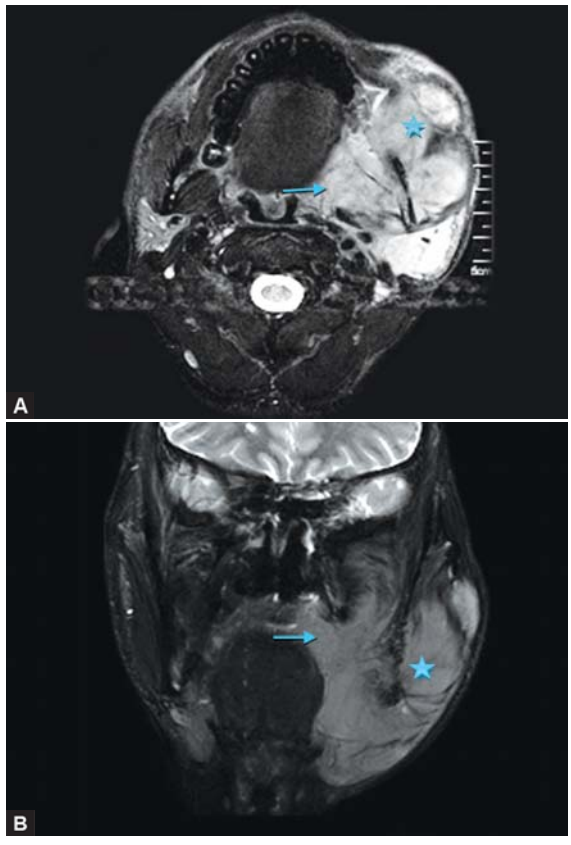

Figs 10A and B: Lymphoma: axial (A) and coronal (B) MRI reveals a large ill-defined homogenously enhancing mass involving the left masticator space (★) and infratemporal fossa (arrow)

soft tissue masses with foci of calcifications within them. Hyperostotic thickening of the involved bone is a common finding. Very rarely a giant aneurysm can erode through the skull base into PPS.

Vascular Lesions

Aneurysms arising from carotid artery, most commonly occur at bifurcation. Preoperative identification of parapharyngeal mass as aneurysm is very important, as surgery can be catastrophic. The presence of characteristic peripheral rim calcification with nonvisualization of ICA separately is adequate for identification of aneurysm.[6] Further confirmation with MRA and CTA can be made.

Internal carotid artery dissection is seen as narrowing of arterial lumen with eccentric mural thickening. CT will also show hypodense intramural hematoma with enhancing rim of vasa vasorum. On MRI intramural hematoma appears hyperintense on both T1W and T2W images. Fat suppressed T1W is the single best MRI sequence for diagnosis of dissection.[21]

IJV thrombosis and ICA occlusions may masquerade as parapharyngeal cystic lesions. However tubular nature of these pathologies, should readily clinch the diagnosis.

Variations in the course of ICA[22] may occur, commonly as a result of atherosclerosis. Close proximity of ICA to pharyngeal tonsils should be reported, as it may increase the surgical risk. Congenital variant of ICA with sigmoid shaped tortuosity can cause bulging of pharyngeal mucosal space, simulating a parapharyngeal or retropharyngeal mass. These variations can be easily identified on contrast-enhanced CT or MRI.

Image-guided Biopsy

Imaging guidance has made it possible to biopsy lesions in the PPS. Ultrasound, which is often used for guided biopsies

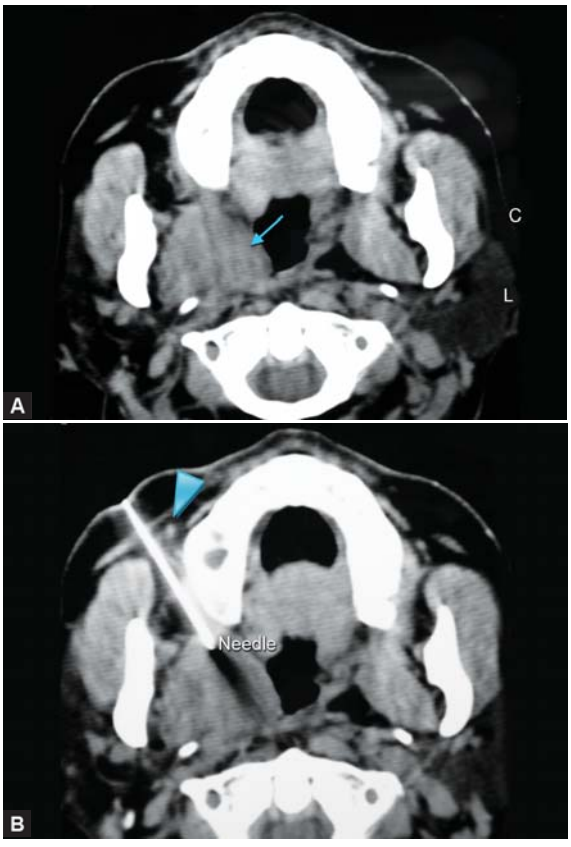

Figs 11A and B: Computed tomography guided biopsy: CT shows an ill-defined mass (A: arrow) in right infratemporal fossa. Needle is directed through paramaxillary approach, lateral to the facial artery (B: arrowhead). It is important to avoid damage to important neurovascular structures by meticulously planning

of superficial lesions, cannot be used here due to poor acoustic window through the overlying bones. CT is the best and most effective to approach deep seated lesions. MRI is not widely used because of the need for special MRI compatible needles, high cost, longer acquisition time and limited availability of open MRI scanners.

Close proximity of structures and overlying bony structures limits the windows for needle trajectory. However, with careful and meticulous planning, it is possible to biopsy almost any parapharyngeal lesion safely (Figs 11A and B). Serious complications are rare, if one is familiar with cross-sectional anatomy and location of major vessels. Also the use of smaller calibre needles reduces the potential of major bleeding. Pain, vasovagal reaction, minor bleeding and infection are some of the minor complications reported with this procedure.[23]

CONCLUSION

CT and MRI are indispensible for the evaluation of PPS and infratemporal fossa. Due to its unique location, pathologies arising in the bordering spaces often secondarily involve the PPS. The pattern of displacement of fat in the PPS helps us to localize the site of origin of the lesion.

ACKNOWLEDGMENT

The authors express their gratitude to Surg Capt IK Indrajit for his valuable contribution.

REFERENCES

1. Som P, Biller H, Lawson W. Tumors of the parapharyngeal space: Preoperative evaluation, diagnosis and surgical approaches. Ann Oto Rhino Laryngol 1981;90:3-15.
2. Harnsberger H. CT and MRI of masses of the deep face. Curr Probl Diagn Radiol 1987;16:143-73.
3. Harnsberger H. The parapharyngeal space and the pharyngeal mucosal space. In: Harnsberger H (Ed). Handbook of Head and Neck Imaging (2nd ed). St. Louis: CV Mosby 1995:29-45.
4. Cummings C, Flint PW, Harker LA. Otolaryngology: Head and Neck Surgery (4th ed). Philadelphia: Elsevier Mosby 2005.
5. Som PM, Brandwein MS, Silvers A. Nodal inclusion cysts of the parotid gland and parapharyngeal space: A discussion of lymphoepithelial, AIDS-related parotid and branchial cysts, cystic Warthin's tumors, and cysts in Sjogren's syndrome. Laryngoscope 1995;105:1122-28.
6. Som PM, Curtin HD. Parapharyngeal space and masticator space lesions. In: Som PM, Curtin HD (Eds). Head and Neck Imaging (5th ed). St. Louis (MO): Mosby 2011;2:2385-2443.
7. Saing H, Lau WF, Chan YF, Chan FL. Parapharyngeal teratoma in the newborn. J Pediatr Surg 1994;29:1524-25.
8. Shin JH, et al. Imaging of parapharyngeal space lesions: Focus on the prestyloid compartment. Am J Roentgenol 2001 Dec;177:1465-70.
9. Batsakis JG, Sneige N. Parapharyngeal and retropharyngeal space diseases. Ann Otol Rhinol Laryngol 1989;98:320-21.
10. Tom BM, Rao VM, Guglielmo F. Imaging of the parapharyngeal space: Anatomy and pathology. Crit Rev Diagn Imag 1991;31:315-56.
11. Anil G, Tan TY. CT and MRI evaluation of nerve sheath tumors of the cervical vagus nerve. Am J Roentgenol 2011 Jul;197(1):195-201.
12. Som P, Biller H, Lawson W. Parapharyngeal space masses: An updated protocol based upon 104 cases. Radiology 1984;153:149-56.
13. Mafee M. Dynamic CT and its application to otolaryngology. Head Neck Surg J Otolaryngol 1982;11:307-18.
14. Furukawa M, Furukawa MK, Katoh K, Tsukuda M. Differentiation between schwannoma of the vagus nerve and schwannoma of the cervical sympathetic chain by imaging diagnosis. Laryngoscope 1996;106:1548-52.
15. Trimas SJ, Mancuso A, de Vries EJ, et al. Avascular carotid body tumor. Otolaryngol Head Neck Surg 1994;110:131-35.
16. Som P, Braun I, Shapiro M, et al. Tumors of the parapharyngeal space and upper neck: MR imaging characteristics. Radiology1987;164:823-29.
17. Vogl TJ, Mack MG, Juergens M, et al. Skull base tumors: Gadodiamide injection-enhanced MR imaging-drop-out effect in the early enhancement pattern of paragangliomas versus different tumors. Radiology 1993;188(2):339-46.
18. Marler JJ, et al. Vascular anomalies: Classification, diagnosis, and natural history. Facial Plast Surg Clin North Am 2001;9(4):495-504.

19. Bauer GP, Volk MS, Siddiqui SY, et al. Burkitt's lymphoma of the parapharyngeal space. Arch Otolaryngol Head Neck Surg 1993;119:117-20.
20. Kawahara N, Sasaki T, Nibu K, et al. Dumbbell type jugular foramen meningioma extending both into the posterior cranial fossa and into the parapharyngeal space: Report of 2 cases with vascular reconstruction. Acta Neurochir 1998;140:323-30.
21. Nusbaum O, Som P, Dubois P, Silvers A. Isolated vagal nerve palsy secondary to a dissection of the extracranial internal carotid artery. Am J Neuroradiol 1998;19:1845-47.
22. Jackel M. Anatomic variants of the internal carotid artery as differential parapharyngeal space-occupying lesions diagnosis. HNO 1997;45:1018-21.
23. Gupta S, Henningsen JA, Wallace MJ, et al. Percutaneous biopsy of head and neck lesions with CT guidance: Various approaches and relevant anatomic and technical considerations. Radio Graphics 2007;27(2):371-90.

ABOUT THE AUTHORS

Sanjay Jain (Corresponding Author)

Head, Department of Radiology, Prince Aly Khan Hospital, Aga Hall, Nesbit Road, Mazagaon, Mumbai, Maharashtra, India e-mail: dr.jainsn@gmail.com

Aman Kumar

Radiologist, Department of Radiology, Prince Aly Khan Hospital Aga Hall, Nesbit Road, Mazagaon, Mumbai, Maharashtra, India

Harshal Dhongade

Radiologist, Department of Radiology, TNMC and BYL Nair Hospital Mumbai Central, Mumbai, Maharashtra, India

Ravi Varma

Associate Professor, Department of Radiology, TNMC and BYL Nair Hospital, Mumbai Central, Mumbai, Maharashtra, India